WMO/TCP/WWW

NINTH INTERNATIONAL WORKSHOP ON TROPICAL CYCLONES (IWTC-9)

Topic 5: Tropical Cyclone Analysis and Remote Sensing

Topic Co-chair:	John Knaff
	NOAA/NESDIS
Email:	John.Knaff@NOAA.gov
Phone:	+1-970-491-8446

Topic Co-chair:	Philippe Caroff
	Meteo France RMSC, La Reunion
Email:	philippe.caroff@meteo.fr
Phone:	+262 262 921106

Rapporteurs: Kotaro BESSHO (JMA), John BEVEN (RMSC, Miami), Thomas MEISSNER (Remote Sensing Systems), Lucrezia RICCIARDULLI (Remote Sensing Systems), Wai Kin WONG (Hong Kong Observatory)

Abstract: In the last four years there has been significant changes in the tropical cyclone community's ability to analyze and diagnose tropical cyclones, which are impacting research understanding and forecast operations. To highlight some of the recent progress, three sub topics are briefly discussed in this report. These subtopics include new and existing methods to estimate TC surface wind structure, next generation geostationary satellites for TC monitoring, and new developments and science using aircraft-based reconnaissance.

5.0 Introduction

This special topic highlights a few developments in the areas of tropical cyclone analysis and remote sensing that have occurred in the last four years.

New capabilities are being tested and demonstrated to increase our ability to estimate surface wind speeds/vectors. Some of these data also have become available to operational forecasters. New techniques include passive L-band (0.5 to 1.5 GHz) based techniques, C-Band (4 to 8 GHz) Synthetic Aperture Radar (SAR), Geographical Positioning System (GPS) reflectometry, and those developed using infrared (IR) imagery. These new techniques nicely complement operational scatterometery and microwave sounder-based methods that continue to improve. Some progress has also been made combining the various estimates to provide improved initial assessments of TC surface wind fields (e.g., TC Vitals). Members have also worked together to make some of these data available with lower latency. The European Space Agency (ESA) and National Aeronautics and Space Administration (NASA), and several research groups have not only developed wind estimate algorithms, but have begun sharing wind speed estimates with operational centres.

In the last four years, two "next generation" geostationary satellite systems have become available (Himawari-8/9 and GOES-16/17), and several similar systems are planned in the next four years. These new satellites provide higher frequency (spectral, spatial, and temporal) observations and present both new opportunities and challenges to forecasters. There are also new capabilities that come with these data, but there are also capabilities that remain unaddressed.

At every IWTC there has been a recommendation of some sort to develop new aircraft reconnaissance-based observational capabilities. Such observations have begun to occur in the western North Pacific region with both low and upper-level aircraft. Observations are being collected and used for operational decisions and in numerical weather prediction models. It is also important to state that three IWTC-8 recommendations are either directly or indirectly addressed in this topic.

5.1 New and Existing Methods to Estimate TC Surface Wind Structure

This subtopic discusses improvements in the ability to estimate surface winds in the hostile environment of TCs. Because most TCs occur over the ocean and are rarely well observed by conventional observations, the methods discussed are based on satellite data. This subtopic covers both methods based on newly available data and those that are based older data and methods where capabilities have improved.

5.1.1 Methods based on newly available data

In the last four years, several methods based on new (to the TC community) data and new methods have become available. These include (1) the L-band passive microwave data from Soil Moisture Active Passive (SMAP) and Soil Moisture Ocean Salinity (SMOS) missions, which were initially designed for soil moisture research, (2) the SAR data, which in the past was difficult to collect, and (3) GPS reflectometry. The time latency of SMOS, SMAP and SAR data are also small enough that wind speeds and vectors should be available to operational centres for evaluation in the next several years.

Passive L-Band data is only minimally affected by rain or frozen precipitation (Wentz, 2005; Reul et al., 2012). L-Band microwave emission from the wind roughened ocean surface is caused by sea-foam (whitecaps) keeps increasing approximately linearly with wind speed (Nordberg et al., 1971; Monahan and O'Muircheartaigh, 1980; Reul and Chapron, 2003; Anguelova and Webster, 2006). This same signal is the basis for visible estimation of surface wind speeds (Neumann, 1952). This signal also remains sensitive to increasing wind even in wind speeds up to 70 ms^{-1}, and the methods used to estimate high wind speeds using SMOS and SMAP data are similar (Reul et al., 2016; Fore et al., 2016; Meissner et al., 2017 and references therein). For wind speeds below 15 ms^{-1}, the performance of L-band radiometers to measure scalar wind speeds is not as good as that of higher frequency radiometers or scatterometers due to larger radiometer noise and lower sensitivity to weaker winds. However, at high wind speeds, particularly above 25 ms^{-1}, L-band radiometers have a distinct advantage over most of these other instruments because they are nearly insensitive to heavy precipitation, show no sign of saturation or sensitivity loss, even in extreme winds. The two downsides to these estimates is their roughly 40 km horizontal resolution and the width of their data swaths, which are relatively narrow. Nonetheless, these sensors are able to provide some of the structural aspects of the highest winds in TCs without aircraft reconnaissance; nicely complementing other techniques that often struggle to estimate the highest wind speeds.

The C-Band SAR systems are the only active microwave sensors able to observe ocean surface night and day and through clouds at high resolution (50 m) with a wide, for this horizontal resolution, coverage (400 km swath). This unique combination can be used to characterize the inner core storm structures, such as, the eye-wall and radius of maximum wind speed, and the rain band locations. Its high resolution also allows measurements in coastal areas without any land contamination. SAR wind measurement principle is thus very similar to scatterometers - it relies on the sensitivity of the backscattered intensity from the ocean sea surface to the ocean surface wind speed and direction. Consequently, most SAR sensors suffered from a decrease in sensitivity for winds higher than 35 ms^{-1}. More recent SAR sensors (Radarsat-2, Sentenal-1), however, have the capability to measure the signal both in co-polarization and cross-polarization (antenna emits in V polarization and receives in H; or vice versa). This improvement provides higher sensitivity to the ocean surface wind speed for extreme winds enables to improve the wind speed accuracy in TCs (Zhang et al., 2012; Horstmann et al., 2015; Hwang et al., 2015). Currently, the impact of rain on measurements of extreme wind is still uncertain and a research topic, but this does not negate the main advantage of these new SAR missions - to infer local information about the TC structure. Finally, thanks to the space component of Copernicus (the European Union's Earth Observation Programme), two SARs (Sentinel-1A and Sentinel-1B) are operational and Sentinel-1C and -1D are planned; ensuring continuity of this data until the end of 2030. As with SMAP and SMOS, the SAR data latencies are being reduced and there are hopes of automating wind speed estimates for TC applications.

Examples of SMAP and Sentinel-1 SAR are shown in Figure 1, where ocean surface wind speed retrievals are compared in Lionrock (2016/08/27). The SAR retrievals follow the algorithm from Mouche et al. (2017) that combines both co- and cross- polarizations to measure ocean surface wind vector at 3-km resolution over TCs and the SMAP algorithm is documented in Meissner et al. (2017).

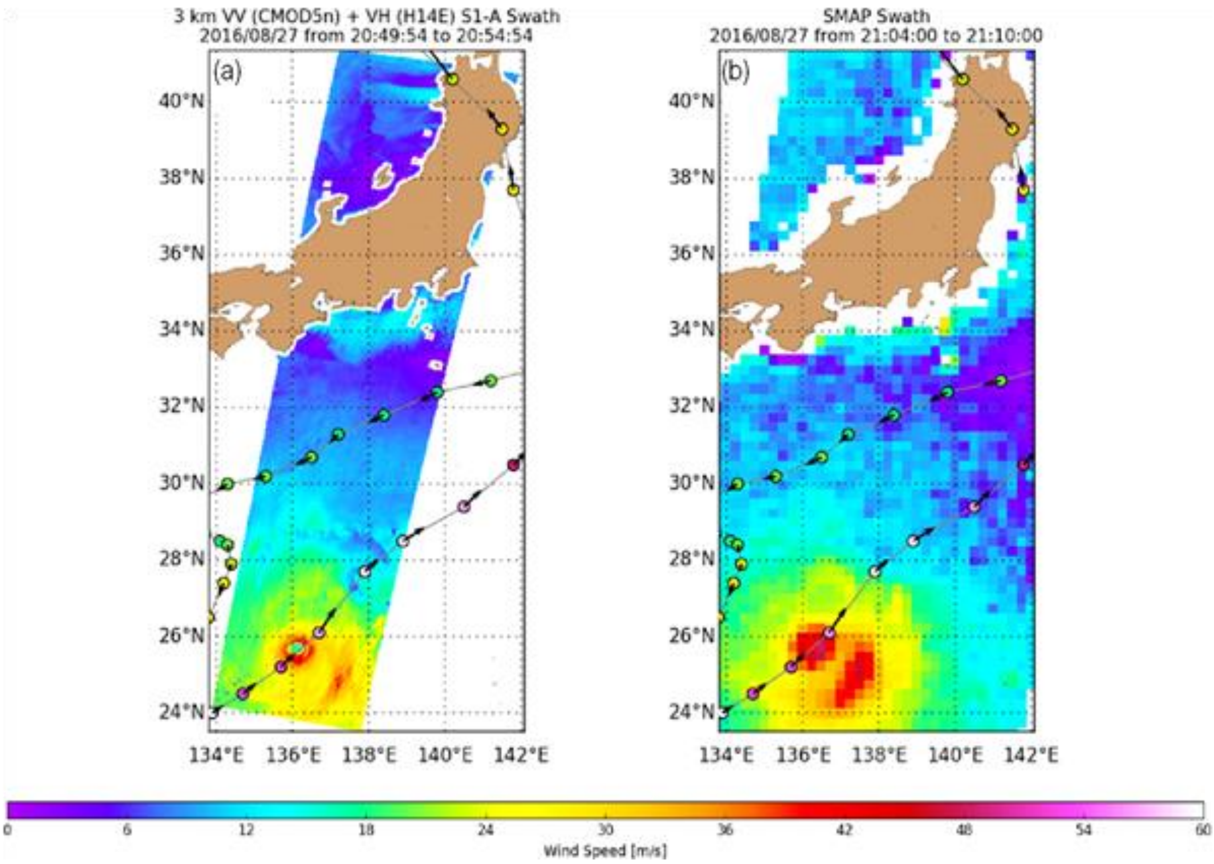

Fig. 1. Wind speed (m s^{-1}) as obtained (a) with SAR using the two polarization channels at 3-km resolution, (b) at 40-km resolution with the SMAP radiometer wind speed from

the RSS algorithm (Meissner et al., 2017). From Mouche et al. (2017).

Global Navigation Satellite System-Reflectometry (GNSS-R) is a remote sensing technique that uses navigation signals—specifically, those that reflect from a surface—opportunistically for science applications (Zavorotny et al., 2014). The Cyclone Global Navigation Satellite System (CYGNSS) is the first science-driven GNSS-R satellite mission. It employs a constellation of eight microsatellites, each with a 4-channel GNSS-R radar receiver capable of measuring GPS Level 1 signals scattered from the surface (Ruf et al., 2016a,b, 2018). CYGNSS provides frequent observations of near-surface ocean wind speed in all precipitating conditions without signal saturation, even in very high wind speeds. The CYGNSS observations of wind speed, appear as single lines that track across the ocean surface corresponding to the GPS reflections between two orbiting satellites (i.e., one CYGNSS and one GPS) during a relatively short period of time.

Using these data, Morris and Ruf (2017a,b) developed methods that objectively estimate TC intensity, wind radii, radius of maximum wind speed, and integrated kinetic energy from simulated CYGNSS Level-2 wind speed estimates. Morris and Ruf's parametric model algorithm, based on Emanuel and Rotunno (2011), smartly interpolates across tracks of CYGNSS observations through a storm, leading to objective estimates of TC metrics. Figure 2 shows a preliminary example of a CYGNSS storm overpass, with the resulting parametric model retrieval. The methods developed in Morris and Ruf (2017b) are currently being applied to on-orbit data. CYGNSS datasets are available about one week following the observations. We expect more GPS-R satellite capabilities will be developed in the next four years, possibly impacting operational interests.

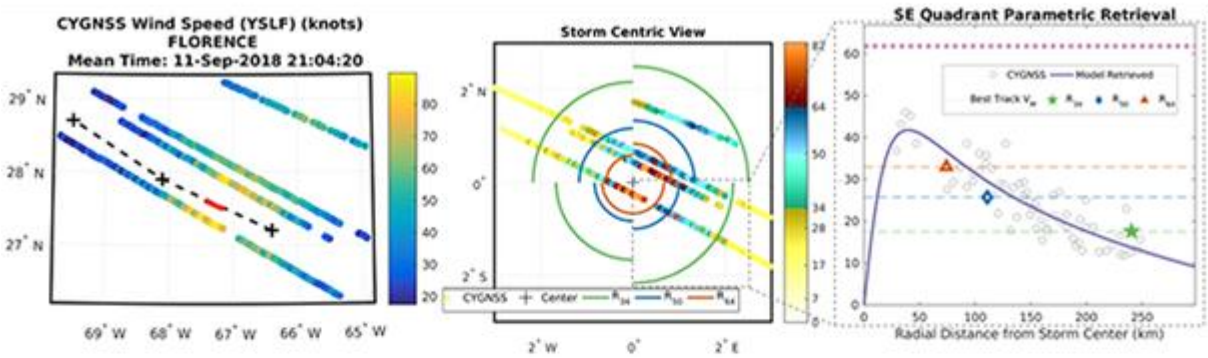

Fig. 2. A CYGNSS overpass of Hurricane Florence on 11 September 2018. Left: In color, CYGNSS YSLF (Young Seas Limited Fetch) wind speed (knots). A dashed-cross line denotes the best track center location, with the red dots denoting the interpolated center position at the CYGNSS coverage time for this plot. Middle: CYGNSS YSLF wind speed, again in knots, but projected in storm centric coordinates, with the closest-in-time best track wind radii estimates visualized for comparison. Right: An example of a CYGNSS parametric model retrieval in the SE quadrant.

5.1.2 Methods based on previously existing data

In this section we review current methods available to estimate surface wind structure. These include, scatterometry, microwave sounder, and IR applications. We ask readers to examine the sub-topic report for a more comprehensive discussion of these methods.

Scatterometry has become a standard for estimating gales. Currently there are three operational scatterometers, SCATSat (India), ASCAT-A (EUMETSAT), and ASCAT-B. The former is a Ku-band (13.515 GHz) and ASCATs are C-band (5.255 GHz). These data are available in real-time from Royal Netherlands Meteorological Institute (KNMI) and others.

Microwave sounders have been updated in the last four years and legacy algorithms, now the Hurricane Intensity and Structure Algorithm (HISA) based on microwave sounder derived temperature and moisture profiles has been created to estimate TC intensity (max winds and minimum sea level pressure) as well as the radial extent of 34-, 50- and 64-knot winds or “wind radii” (Chirokova et al., 2017; Demuth et al., 2004, 2006; Bessho et al., 2006). Microwave Integrate Retrieval System (MIRS) – based 3-D profiles of temperature, moisture and cloud liquid water called the Microwave Integrated Retrieval System (MIRS) (Boukabara et al., 2013).

In the last four years, a couple of methods to estimate gales via information provided by IR imagery have been developed. These include the method documented in Dolling et al. (2016), that makes use of the deviation angle variance (DAV) technique (DAV-T; Piñeros et al., 2008) combined with sea surface temperature, TC age, and current intensity, to estimate wind radii. Similarly, Knaff et al. (2016) uses IR based estimates of TC size (Knaff et al., 2014), TC motion and current intensity to estimate wind radii. This latter is method is used at Joint Typhoon Warning Center (JTWC), where operational Dvorak intensity/center fixes provide inputs, and in the latest version of the Advanced Dvorak Technique (Velden and Olander, 2018).

Finally, to help forecasters put all this TC structure information together, JWTCuses a recently developed objective wind radii best tracking (OBTK) procedures. OBTK combines several estimates of current surface wind structure including forecaster-estimated, satellite-based-automated-objective estimates, and six-hour model-forecasts. OBTK estimates of gales have mean absolute errors of roughly 15% when compared to ASCAT wind radii (Sampson et al. 2017, 2018). OBTK calculations are performed on the Automated Tropical Cyclone Forecasting (ATCF; Sampson and Schrader, 2000). ATCF is also used at NHC and The Central Pacific Hurricane Center. More information can be found the sub-topic 7.2 report (Meissner et al., 2018).

5.2 New generation geostationary satellites for TC monitoring

In the last four years, several next generation satellites were launched by member states and have become operational. These include the Japanese Himawari-8, and Himawari-9 (spare), the United States of America's GOES-16 (GOES-EAST) and GOES-17 (GOES-WEST replacement). There are also several next generation geostationary satellites that will become operational in the next four years including China's FY-2, Korea's GeoKOMPSAT-2A, and EUMETSAT's MTG, which have similarly improved imager features. These functions and specifications are notably improved from those of the imagers on the previous satellites. Some of the satellites also have or will have optical lightning mappers and hyperspectral infrared sounders. These four years have also allowed researchers and forecasters to use and exploit these new capabilities. Below we briefly discuss how these data have been used to aid decision making, advance applications, and improve TC analysis and forecast guidance. More details can be found in the subtopic 7.2 report (Bessho et al., 2018).

5.2.1 Improved decision making

With the new capabilities of these next generation geostationary satellites, namely improved temporal sampling, spectral resolution (i.e., number of channels), spatial resolution, and navigation, these satellites lend themselves to improved decision making.

Center fixing is improved primarily by the higher temporal and spatial resolutions, but also aided by the different visible and near-IR channels. Center determination is further aided by special rapid scan operations and improved navigation. Reducing errors in location lead to improved assessment of geneses/formation potential, intensity and structure, and Numerical Weather Prediction (NWP) initialization. Continuous TC genesis assessment is also aided as important features like subtle changes in outflow boundaries, are more easily tracked. Therefore, while the methods have not changed dramatically, the available information has improved in quantity and quality, in some cases dramatically.

Routine subjective Dvorak analyses are either being replaced or supplemented by objective techniques (Olander and Velden, 2018; Kishimoto et al., 2013). The increased resolutions have, in some cases, increased the intensity estimates, as the eye is viewed as being warmer. JMA is now using spatial average of eye temperature instead of the warmest eye pixel to adjust for the higher eye temperatures. However, the increased temporal resolution is greatly beneficial, generally resulting in better scene identification, improved center location, and more frequent observations, especially in the Southern Hemisphere. The more frequent observations also lend themselves to temporal averaging, which acts to reduce noise and increase accuracy.

Multiple visible, near-IR, and water vapor channels have also improved analyses. The co-viewing of visible and near-IR channels helps discriminate the phase and thickness of cloud features, allowing improved interpretation and, in particular, better discrimination of low-level clouds, as shown in Fig. 3. Similarly, the multiple water vapor channels provide a poor man's water vapor sounder, allowing for the local tracking of dryer air masses, when animated, and vital information about how water vapor is distributed/stratified vertically.

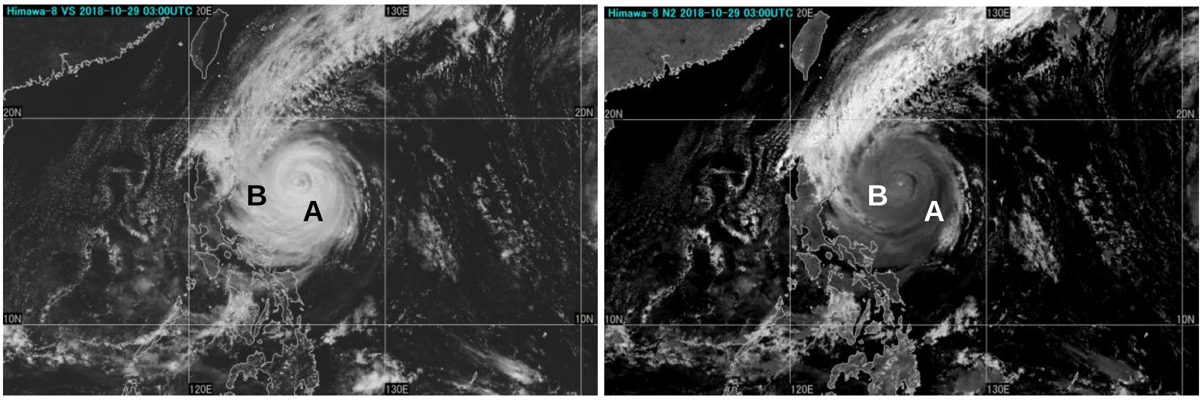

Fig. 3. Comparison of VIS (left) and NIR (right) imagery of Typhoon Yutu (2018) as viewed by Himawari-8. Notice how the eyewall region appears much darker in the NIR (A) and that the low-level (non-frozen) clouds appear much brighter in the NIR image at the low to high cloud transition point (B).

5.2.2 Advanced Applications

The newer generation of geostationary satellites, Meteosat Second Generation, GOES-16/17, and Himawari 8/9 has led to wider use of Red Green Blue (RGB) image combinations to display satellite imagery. RGB combinations have been created to aid the tracking of temperature and water vapor in the atmosphere, cloud top microphysics and water phase, provide cloud top pressures/heights and better detect surface features. Advanced workstations can overlay model output/analyses and conventional data on top of this imagery to further increase information content. These RGB combinations are in use at most RSMCs, though there does not seem to be a consensus set of products or usage. While strictly not an RGB, the Saharan Air Layer product, with GOES-16 and 12-μm imagery, can now be produced again.

Navigation, spatiotemporal, and spectral resolution have all increased with the next generation geostationary satellites. Each of these plays a role in improving Atmospheric Motion Vectors (AMVs). The availability of multiple water vapor channels helps with tracking of mid-level cloud motions, the higher precision near infrared and infrared channels are being used to track low-level features at night and provide better height assignments. The high-resolution visible imagery is also being used to track fine-scale features during daylight hours. These higher quality AMVs are being used in research and operations. Operationally, JMA is using near-surface AMVs to provide surface wind estimates and help with tracking and estimates of gales (Fig. 4), while NHC is just starting to utilize these new capabilities. Research has also been investigating the relationships between cyclonic outflowing winds and TC intensity, showing that the latter is highly correlated to the maximum tangential wind of upper tropospheric AMVs (Oyama et al., 2018). The higher quality AMVs are also making their way into models via data assimilation (section 7.2.3). New methods, like optical flow algorithms are also being tested for AMV estimation.

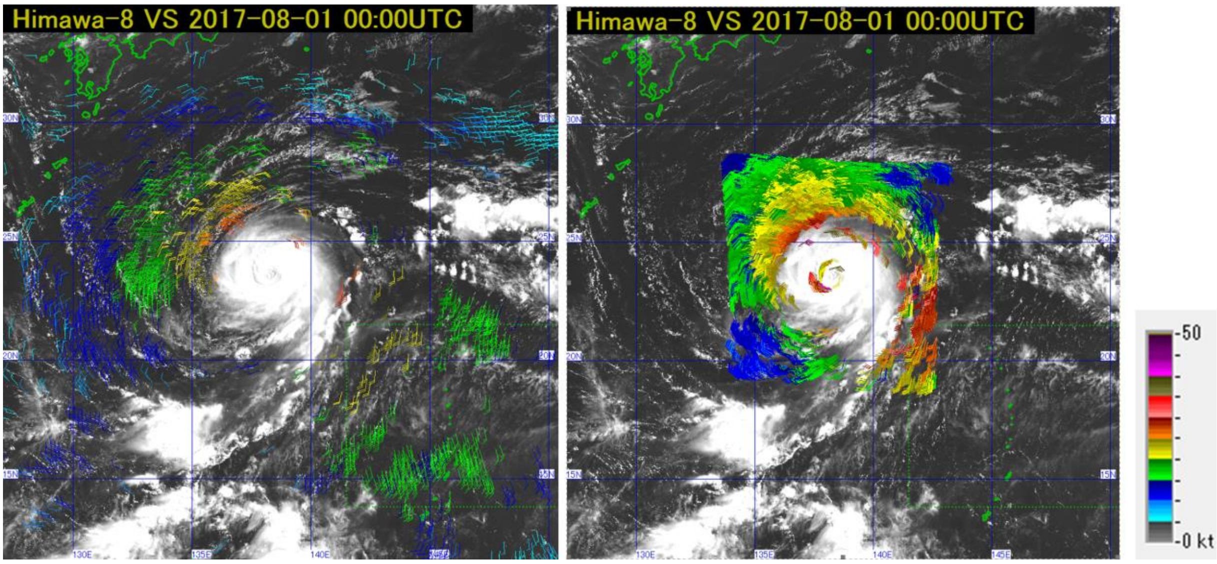

Fig. 4. The surface AMVs (colored arrows) retrieved from Himawari-8 imagery of Full-Disk (left) and target area (right) at 00:00 UTC 1 August 2017 for Typhoon Noru. Background is a Band 3 (0.64 μm) Visible image. The color of arrows indicates the wind speed (kt).

GOES-16 and GOES-17 also have incorporated a new instrument: The Geostationary Lightning Mapper (GLM). The GLM allows forecasters to continuously monitor total lightning (cloud-to-ground + intracloud) in TCs beyond the range of current ground-based lightning detection networks with a high detection efficiency (Goodman et al., 2013). Prior research using ground-based networks (mostly cloud-to-ground) showed that lightning can help improve intensity forecasts (DeMaria et al., 2012). Stevenson et al. (2018) also showed intense lightning activity is often associated with deep active convection, which favors TC intensification when located within the radius of maximum wind. The GLMs are relatively new and NHC forecasters have only recently gained access to GLM data from GOES-16 on their operational workstations. Given the prior work with ground-based lightning, the GLM is expected to help TC forecasters, and be used by the research community.

5.2.3 Data Assimilation Efforts

With the tremendous investment in geostationary satellites, much effort has been spent trying to assimilate AMVs and radiances in hurricane models. Results from such studies are optimistically showing generally that AMVs and radiance data assimilation helps the initial state estimate and can lead to improved forecasts. Given the lack of other data where TCs form, such activities have enormous potential returns, but data assimilation in the hurricane scene remains a difficult task as TCs are extreme phenomena with heavy rainfall, highly curved inflowing and outflowing winds, and dense cloud cover. In the TC environment, both new/improved data treatment techniques and more sophisticated NWP methods are required to have the most successful data assimilation and forecast improvement outcomes. We ask the reader to review the report Bessho et al. (2018) for more information.

5.2.4 Coming capabilities of future geostationary satellites

The capabilities of emerging and near-future geostationary meteorological satellites are quite promising. China’s FY-4 series (the first satellite was launched in 2017) includes a hyperspectral IR sounder and a lightning mapper. The payloads of the Meteosat Third Generation satellites also plan to include a hyperspectral sounder. The U.S. GOES-R series will continue with the launches of GOES-T and –U. However, GOES-T and –U will be delayed as the cooling system needs to be upgraded. These satellites will carry the GOES-16/17 legacy instruments which include the high-resolution imager (i.e., the Advanced Baseline imager) and lightning mapper (i.e., GLM). Korea plans to launch its new Kompsat series -2A and -2B, with much improved imagers and a hyperspectral sounder on -2B. India will also launch Insat-3DS that will continue the successful Insat-3 series. Finally, JMA is designing the Himawari-8/9 replacement and expect to begin manufacturing in 2023 with operations set to begin in 2029.

Of these future capabilities, hyperspectral sounders may be a topic at the next IWTC, as they provide superior precision and higher temporal frequencies and may be able to better depict the rapidly changing conditions associated with TC environments. Eye soundings may also be possible in TCs with cloud-free eye structures.

5.3 New developments and science using aircraft-based reconnaissance

It has been a recurrent recommendation of past IWTCs to call for an extension of regular and coordinated aircraft reconnaissance missions in other TC basins than those covered by the long-standing U.S. program. We are happy to report that in recent years there has been significant progress toward this goal in the western North Pacific. In the last four years, new airborne observational technology has also emerged, and refined strategies for designing optimal aircraft flight patterns meant to maximize the impact of these observations on NWP-based forecasts of track and intensity have been tested. Below we provide an overview of the current status of airborne observing technologies and strategies, highlight some applications of these aircraft-based observations to improve analysis of TC intensity and structure, and discuss what efforts are planned in the future. All details will be found in the subtopic 7.3 report (Wong et al., 2018).

5.3.1 TC aircraft reconnaissance and field campaigns

5.3.1.1 Advances in the U.S. aircraft reconnaissance program

The U.S. TC scientific community, and in particular the National Oceanic and Atmospheric Administration (NOAA), continues to improve and update its airborne capabilities designed to make in-situ observation of TCs. To this end, new observation platforms or instruments have been recently tested.

New platforms include large and small Unmanned Aerial Vehicles (UAVs) such as NASA's Global Hawk and unmanned aerial systems (UASs) like the Coyote (Cione et al., 2016). The Global Hawk, an unmanned aircraft for high-altitude, long-duration Earth science missions, has been used in several TC field campaigns. The Coyote, on the other hand, is a small remotely-piloted device launched from dropsonde tube on the WP-3D aircraft that is able to fly and make observations at very low altitudes, where manned aircraft cannot fly. Such capability allows the Coyote to be used for a real-time assessment of near-surface/boundary layer winds and minimum sea level pressure. Coyote UASs were successfully deployed in Hurricanes Edouard (2014) and Maria (2017). Further development of the Coyote technology is ongoing. Those efforts will add additional instrumentation, and extend the flight duration (now being only 1 to 2 h).

Among the full array of instruments and devices deployed or operated on U.S. weather reconnaissance aircraft are floats and profilers for oceanic sampling, Tail Doppler radar, for 3-D winds and rain rate, the SFMR (Stepped Frequency Microwave Radiometer), for surface wind speed and rain rate, and the dropsondes. One of the more exciting observational capabilities is the addition of the Wide-swath Scanning Radar Altimeter

(WSRA), which can provide near-real-time reporting of ocean directional wave spectra, significant wave height, rain rate, and the mean square slope of the ocean surface. It is also noteworthy that older NCAR/Vaisala RD-94 dropsondes are now being replaced by the newer/better designed NCAR/Vaisala RD-41 dropsondes.

One of the new instruments, the Doppler Wind LIDAR (DWL), detects and tracks the relative movement of aerosols via laser light and provides wind vectors in regions where there is a lack of precipitation scatterers. As such, the DWL provides a complement to wind measurements obtained with the tail Doppler RADAR, which is reliant upon precipitation scattering. Such capability can prove valuable in situations with pronounced precipitation asymmetries, such as TCs in vertical wind shear (Zhang et al., 2018) and/or for improved boundary layer wind observations.

Concurrent with these steady technology improvements, innovative strategies are being tested to take the most advantage of the whole set of aircraft-based observations. A new targeting strategy for the aircraft flight planning discussed in Torn (2014) was tested during reconnaissance flights associated with Hurricane Michael (2018) and Central Pacific Major Hurricane Lane (2018), before being implemented operationally for the first time in Hurricane Florence. The strategy relies on the computation of numerical model uncertainty fields based on ensemble model output (from the EC model). The flight tracks are then designed to sample coherent regions where there is the maximum uncertainty. It still remains to be demonstrated if this strategy systematically reduces model uncertainty and thus improves forecasts.

The philosophy and motivations of the NOAA's airborne sampling program for TCs is contained within the NOAA Intensity Forecasting Experiment (IFEX; Rogers et al., 2006, 2013) which aims at tackling the challenge of intensity forecasting, particularly for rapid intensity change events. Through IFEX, significant advances have been made in the real-time display of aircraft data for NHC forecasters. Analyses of reflectivity and winds from the tail Doppler radar are now available within approximately 20 minutes following the completion of the aircraft's pass through the TC center. These observations can also be accessed online like the example shown in Fig. 5.

In 2018, and for the first time, real-time Doppler radar analysis data has been ingested into the software that NHC forecasters use to visualize TC structure as they prepare their forecasts. This data can now be co-viewed and combined with other data sources, e.g., from GOES-16, to provide forecasters an unprecedented look at the TC inner-core and to assess features such as deep convection, vortex tilt, radius of maximum wind or the presence of secondary eyewalls (Fig. 6).

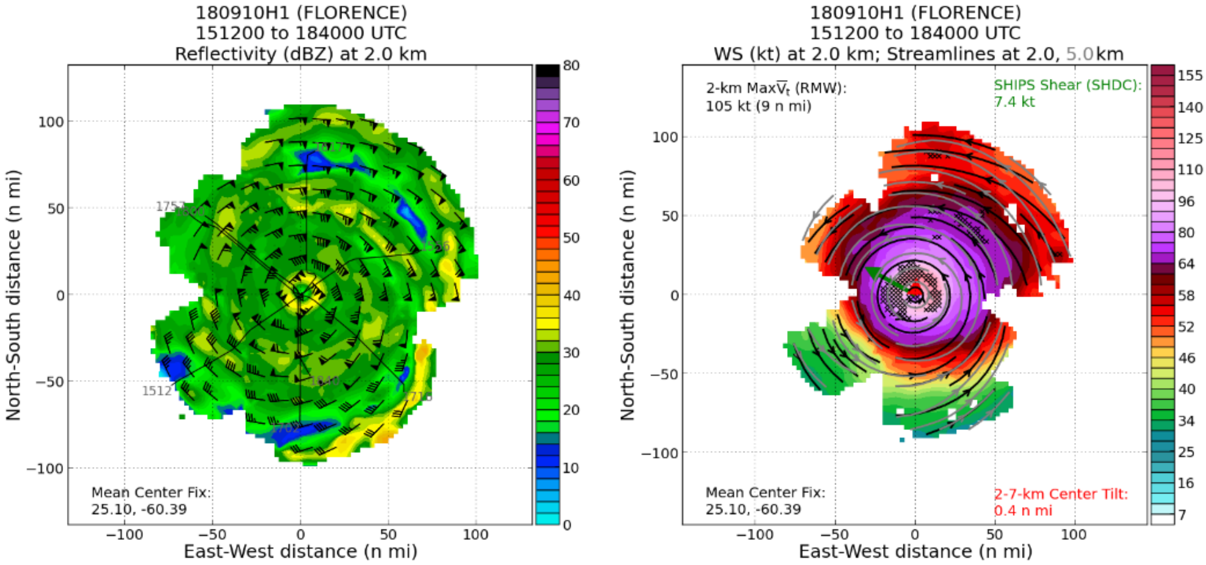

Fig. 5. Real-time tail Doppler radar analyses from Hurricane Florence (2018). (a) Reflectivity (shaded, dBZ) and winds (barbs, kt) at 2 km altitude sampled during 1512-1840 UTC 10 Sept.; (b) As in (a), but for wind speed (shaded, kt), streamlines at 2 km (black) and at 5 km (grey) altitude, and radar-derived diagnostics in text. Black x's in (b) denote locations where the peak vertical velocity in the 4-16 km layer is > 1 ms^{-1}.

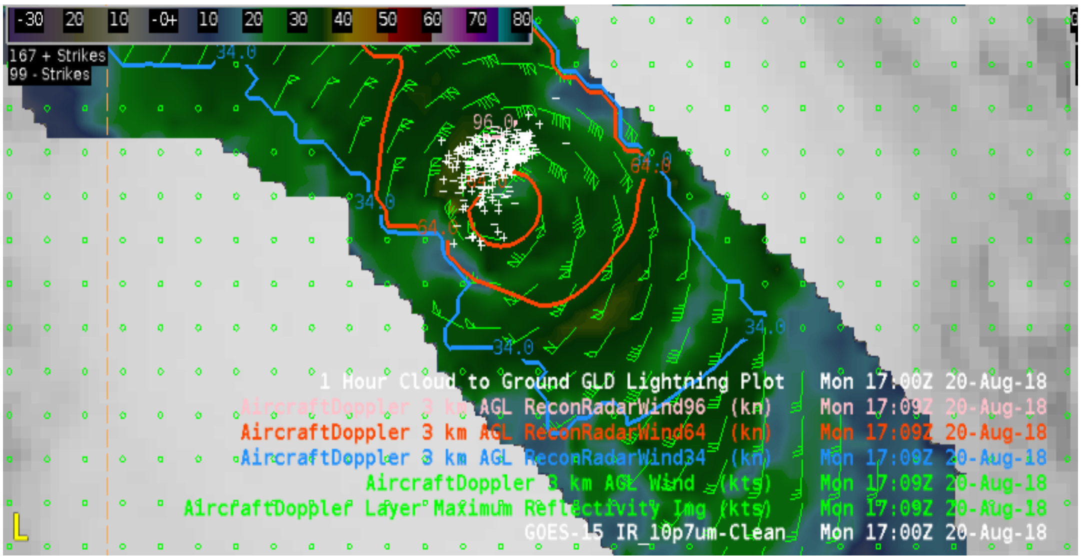

Fig 6. Image in Advanced Weather Interactive Processing System (AWIPS)-II showing 3-km winds (barbs, kt), layer maximum reflectivity (shaded, dBZ), 34- (blue) and 64- (red) kt wind contours at 3 km and 1709 UTC 20 August, and GOES-16 infrared image and locations of GOES-16 measured cloud-to-ground lightning strikes (white "plus" and

“minus” signs) at 1700 UTC in Hurricane Lane (2018) (courtesy Stephanie Stevenson, NHC).

5.3.1.2 Aircraft reconnaissance advances in the North-West Pacific

A pioneering program for aircraft-based Typhoon surveillance missions in the western North Pacific was the Dropwindsonde Observations for Typhoon Surveillance near the Taiwan Region (DOTSTAR) program. Starting in 2003, DOTSTAR has investigated 63 typhoons in 2017 (conducting 79 flights and releasing 1291 dropsondes). The targeted observations conducted by DOTSTAR have resulted in a robust (10 to 20%) improvement in model forecasts of typhoon tracks in both the National Center for Environmental Prediction’s (NCEP) Global Forecast System and European Center for Medium Range Weather Forecasts’ (ECMWF) Integrated Forecast System (Chou et al., 2011) and has shed light on typhoon dynamics. DOTSTAR was an active partner of the Tropical cyclone-Pacific Asian Research Campaign for Improvement of Intensity estimations/forecasts (T-PARC) field campaign conducted in collaboration with Japan and the United States of America, and more recently (2017-2018) in the T-PARC-II campaign. The T-PARC project, funded by Japan for the 2016-2020 period, aims to improve estimations and forecasts of TC intensity as well as storm track forecasts. For T-PARC-II, a new dropsonde and multi-channel receiver has been developed with very light weight and without the parachute. A newer version of this light weight dropsonde that uses more environment-friendly materials is currently under development.

Hong Kong, China, has also joined the global regional aircraft reconnaissance effort. In collaboration with the Government Flying Service (GFS), Hong Kong Observatory (HKO) commenced reconnaissance flights for TCs over the northern part of South China Sea in 2011, providing high-resolution wind, temperature and relative humidity data along the flight paths (Chan et al., 2011). The flight-level observations were used to analyze the TC position, intensity and structure in a near-real-time manner. These observations also contributed positively to TC forecast track improvements in the next 2-3 days, as well as improved analysis and forecast of TC structure in a mesoscale NWP model (Wong et al., 2013). In 2016, a dropsonde measurement system was installed on board a new jet GFS aircraft. Since the first mission, about 20 flights have been conducted. The near-real-time dropsonde observations were disseminated using the GTS. HKO has also contributed to the TC surveillance flight data acquisition in various international and regional projects, including T-PARCII and the Experiment on Typhoon Intensity Change in Coastal Areas (EXOTICCA), among others. An example of how these dropsonde data from different field projects can be combined is shown in Fig. 7, where DOTSTAR and HKO’s dropsondes are combined in an analysis.

EXOTICCA started in 2014 being coordinated by the Shanghai Typhoon Institute of China Meteorological Administration (STI/CMA) and HKO. The major objectives of EXOTICCA are to conduct: (a) field campaigns on the intensity and structure characteristics of the target offshore and landfalling TCs using integrated and novel observation techniques; and (b) demonstration research on the utilization of the synergized field observation data with the aim of deepening the understanding of the mechanism of structure and intensity changes, to improve the relevant capability of operational analysis, NWP model forecasts, reliable storm surge and flooding and associated risk assessment (Lei et al., 2017).

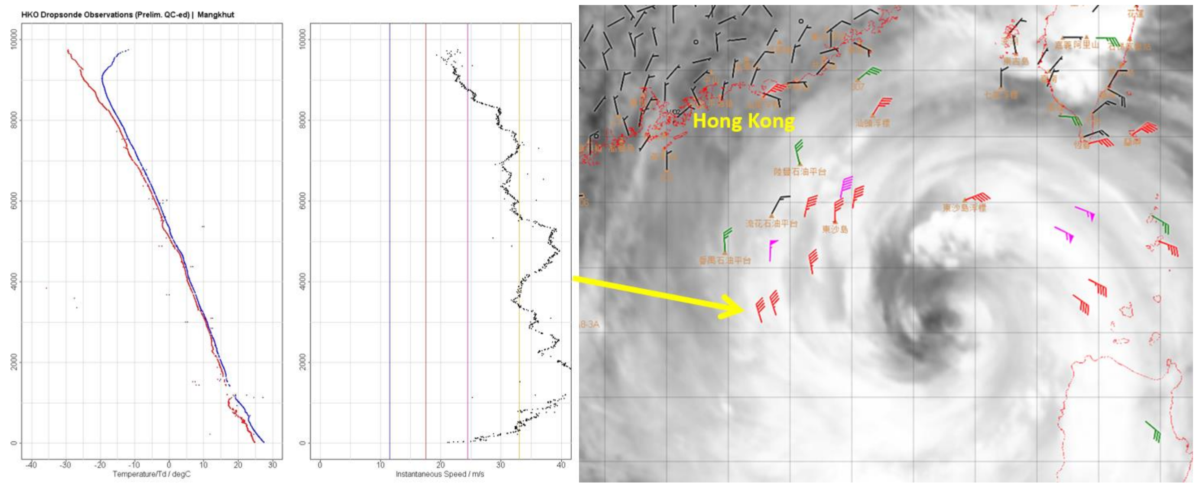

Fig. 7. Near-surface winds[knots] sampled within the circulation of Typhoon Mangkhut on 15 September 2018 by dropsonde missions conducted by HKO (northwest quadrant) and DOTSTAR (northeast quadrant) together with other surface wind observations.

Several new observation platforms have been implemented by STI/CMA during the observational field campaign experiments, including low-altitude/lower boundary layer (400-600m) UAV observations of winds and temperatures. In order to obtain in-situ observations of the TC structure, particularly the vertical profiles of wind, temperature, pressure and moisture of the inner-core or in different quadrants of the storm at same time, a "rocket-dropsonde" system was also developed by STI/CMA. This system uses a rocket platform to release dropsondes over targeted areas. The positions of dropsondes are determined by the Beidou satellite, which also transmits the dropsonde observations to the ground operation centre. This rocket-dropsonde system was used to investigate Severe Typhoon Mujigae in October 2015. The rocket was launched from Hainan Island, about 330 km west-southwest to the center of Mujigae and four dropsondes were released in the periphery of Mujigae's inner-core. Nearly simultaneously, HKO conducted a surveillance flight, passing through the centre of Mujigae a little earlier. This collaborative operation provided a valuable opportunity to validate the airborne observations of the typhoon from different platforms or techniques and to analyze the inner-core structure of Mujigae (Fig. 8).

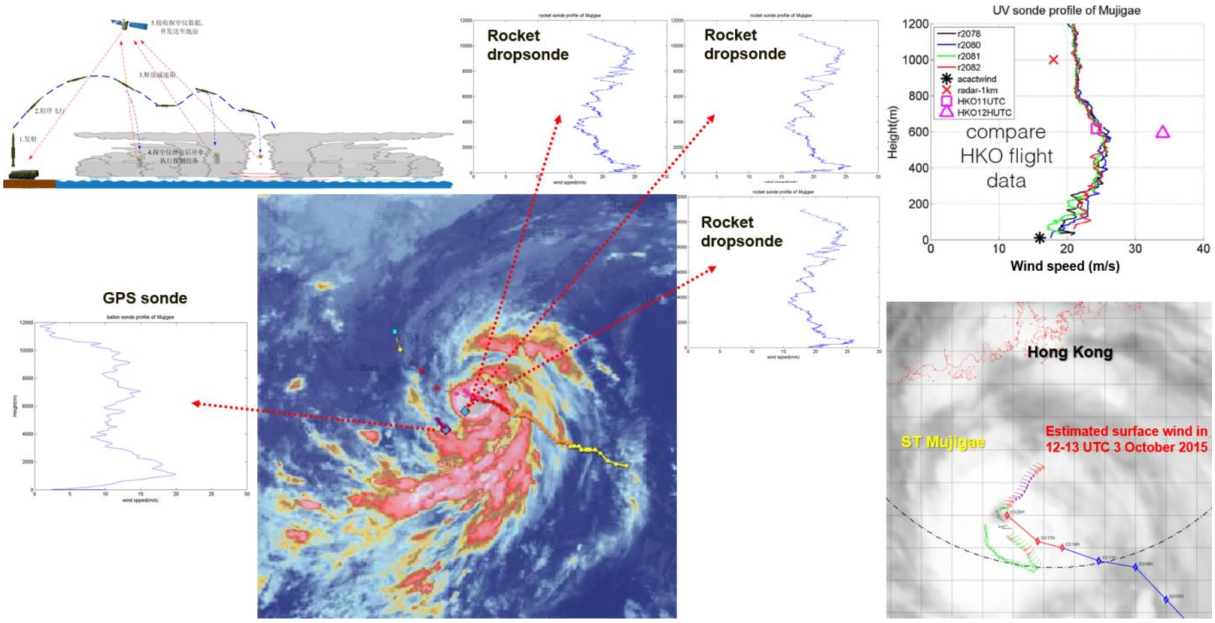

Fig. 8. The schematic of rocket-dropsonde (top left) and vertical profiles of wind speed [ms^{-1}] collected around ST Mujigae by STI/CMA on 3 October 2015. Comparison of wind profile of rocket-dropsonde versus those collected by the HKO reconnaissance flight (top right), and estimated surface winds along the HKO reconnaissance flight's path (bottom right).

5.3.2 Applications of aircraft-based observations

5.3.2.1 Collecting observations that span the TC life-cycle in a variety of environments for model initialization, sensitivity studies and evaluation

Many of the IFEX missions have targeted TCs in the early stages of their life-cycle, as this has the potential to capture many important features in a TC's intensity evolution, including genesis and rapid intensification. The data collected in these missions are used to improve TC intensity forecasting in several ways. First, data is transmitted in real-time to the NOAA Environmental Modeling Center (EMC), where it is assimilated into the operational regional Hurricane Weather Research and Forecasting (HWRF) model. Earlier efforts were successful in developing the capability of transmitting airborne Doppler radar data in real-time to EMC. Those efforts showed some success in reducing forecast error when those data were assimilated into the Weather Research and Forecasting (WRF) model. There are many recent studies that show that forecast errors can be reduced by assimilating/using aircraft data, including flight-level observations, dropsonde observations, and airborne Doppler RADAR-based wind estimates (Zhang and Weng, 2015; Aberson et al., 2015; Weng and Zhang, 2016; Tong et al., 2018). Similarly, dropsondes from the Global Hawk UAV have also been shown to improve TC analyses and forecasts (Christophersen et al., 2017, 2018a,b).

Another way aircraft data improves TC intensity forecasting is by facilitating model evaluation, which can lead to improvements in the representation of physical processes in the model (Zhang et al., 2013a,b). The impact of using observations to improve the representation of vertical eddy diffusivity was shown in Gopalakrishnan et al. (2013) and Zhang et al. (2015, 2017). Using this improved eddy diffusivity results in a shallower and stronger TC boundary layer inflow layer, more consistent with observations, as well as differences in other boundary layer properties such as stability, convergence, and angular momentum advection. These changes have been shown to produce better forecasts of rapid intensification (Zhang et al., 2017), as well as providing a better representation of TC size (Bu et al., 2017). Zhang et al. (2018) used aircraft observations to reduce the horizontal mixing length in HWRF forecasts of Hurricane Earl and found that many structural aspects were improved, including storm size, boundary layer heights, warm-core height, and eyewall slope. Biases in both storm intensity and storm size were significantly reduced with the modified horizontal mixing length.

It is also important to mention that these manned aircraft, UAV and UAS based data are critical for development of satellite-based techniques. For instance, there are few conventional observations of extreme winds from which SMOS, SMAP, SAR and GPS-R methods can be validated against. So aircraft-based data remain critical for nearly every aspect of TC research, development and forecasting.

5.3.2.1 Improve the understanding of physical processes driving intensity changes of a TC at all stages of its life-cycle

The third IFEX goal is primarily concerned with hypothesis-driven research aimed at better understanding intensity change processes within the TC inner core and its environment. Much of the recent work has focused on the TC response to vertical shear and the structure and distribution of precipitation and its relationship to TC intensity change. The understanding gained from these observationally-based studies is being used to guide the development of forecasting tools and model improvements that hold the potential to improve TC intensity forecasts. For more details on this topic refer to topic 5.3 report, Wong et al. (2018).

5.4 Recommendations

1. Support the growing number of research and operational programs that are providing accurate validation data for satellite-derived surface wind speeds/vectors outside the Atlantic TC basin. Including validation of new observational capabilities (how good?) and the real-time sharing and exchange of aircraft/UAV –based observational data. (for WMO)
2. Support efforts to make current and future research and development satellite data and products available in real-time or near real-time to permit operational applications after successful cal/val. (for WMO)
3. We recommend further investigation of the use of GNSS-R data for determining TC size, strength and structure. (for Researchers)
4. Encourage the use and evaluation of wind fields from L-band radiometers (SMOS and SMAP) for determining intensity and 34-, 50, and 64 kt radii in TC. (for Forecasters and Researchers)
5. Encourage the use and evaluation of SAR-derived ocean surface wind speeds. These complement other techniques, but provide invaluable inner-core wind structure information. (for Forecasters and Researchers)
6. Encourage the global community to collaborate on the optimal mix of legacy satellite sensors along with those coming from small satellites and CubeSats. (for WMO)
7. To encourage and support for another International Workshop on Satellite Analysis of Tropical Cyclones (IWSATC) in the near future; expanding the role to better reach underdeveloped TC-prone countries. (for WMO)
8. To support/continue to support the development of new aircraft observation platforms such as dropsondes, UAS/UAV, RADAR/LIDAR instruments on board the flight vehicles and provide quality observations with high resolution in both space and time (for WMO, and researchers)
9. To support technique development and applying aircraft observations in analysis of TC intensity, wind distribution, boundary layer structures during the whole TC lifecycle (to researchers)
10. Support enhanced nowcasting and/or forecasting techniques of TC intensity, rapid intensity change and associated high-impact weather using combinations of the aircraft reconnaissance-based data, satellite-based data, other meteorological observations (for WMO, Forecasters and Researchers)
11. Support the application of new aircraft observational data for data assimilation activities in NWP models, for improving model physics in those models, and for improved validations of model output and physical processes (for Researchers)
12. Document (and/or through training opportunities) how aircraft (new and old) can be used by RSMC/TCWC forecasters to improve their analysis of TC intensity and surface wind structure, and leading to more accurate, effective assessment or

communication of uncertainty of potential impacts to the users and general public (to WMO and Forecasters)

13. To support / organize coordinated field campaigns of various aircraft observation missions and experiments for gathering observation datasets of the whole TC lifecycle and intensity evolution (to WMO)

Acknowledgments:

The Topic Chairs would like to thank our Rapporteurs Kotaro Bessho, Jack Beven, Thomas Meissner, Lucrezia Ricciardulli, and Wai Kin Wong and their team members for their great work and help with this topic. We also thank our organizations (NOAA, Meteo France, Remote Sensing Systems, JMA, and the Hong Kong Observatory) for allowing us time to complete the work.

Acronyms used in the report:

AMV	Atmospheric Motion Vector
ATCF	Automated Tropical Cyclone Forecast system
AWIPS-II	Advanced Weather Interactive Processing System-II
CYGNSS	Cyclone Global Navigation Satellite System
DAV	Deviance Angle Variance
DOTSTAR	Dropwindsonde Observations for Typhoon Surveillance near the Taiwan Region
DWL	Doppler Wind LIDAR
EMC	Environmental Modeling Center (USA)
ESA	European Space Agency
EXOTICCA	Experiment on Typhoon Intensity Change in Coastal Areas (China)
GFS	Government Flying Service (China)
GLM	GOES Lightning Mapper
GNSS-R	Global Navigation Satellite System-reflectometry
GOES	Geostationary Operational Environmental Satellite
GPS	Global Positioning System
GTS	Global Telecommunications System
HISA	Hurricane Intensity and Structure Algorithm
HKO	Hong Kong Observatory
HWRF	Hurricane Weather Research and Forecasting model
IFEX	Intensity Forecasting Experiment (USA)
IR	Infrared
IWTC	International Workshop on Tropical Cyclones
JMA	Japanese Meteorological Agency

JTWC	Joint Typhoon Warning Center
LIDAR	Light Detection and Ranging
KMNI	Royal Netherlands Meteorological Institute
MIRS	Microwave Integrated Retrieval System
NASA	National Aeronautics and Space Administration
NCAR	National Center for Atmospheric Research (USA)
NOAA	National Oceanic and Atmospheric Administration
NWP	Numerical Weather Prediction
OBTK	Objective Best Track
RADAR	Radio Detection and Ranging
SAR	Synthetic Aperture Radar
SFMR	Stepped Frequency Microwave Radiometer
SMAP	Soil Moisture Active Passive
SMOS	Soil Moisture Ocean Salinity
STI/CMA	Shanghai Typhoon Institute of China Meteorological Administration
UAS	Unmanned Aerial System
UAV	Unmanned Aerial Vehicle
WRF	Weather Research and Forecasting model
WSRA	Wide-swath Scanning Radar Altimeter
YSLF	Young Seas Limited Fetch

References:

Aberson, S. D., K. J. Sellwood, and P. A. Leighton, 2017, Calculating Dropwindsonde Location and Time from TEMP-DROP Messages for Accurate Assimilation and Analysis. J. Atmos. and Ocean. Tech., 34, 1673-1678.

Anguelova, M., and F. Webster, 2006, Whitecap coverage from satellite measurements, A first step toward modelling the variability of oceanic whitecaps, J. Geophys. Res. 111(C3), DOI:10.1029/2005JC003158.

Bessho, K., J. L. Beven, A. Burton, J. Courtney, M. Folmer, J. Kerkmann, S. Nishimura, K. Okamato, A. Schumacher, and C. Velden, 2018, Subtopic 7.2: New generation geostationary satellites for TC monitoring. WMO International Workshop on Tropical Cyclones - 9, Honolulu, HI, USA, 3-7 December, 16pp

Bessho, K., M. DeMaria, and J. A. Knaff, 2006, Tropical Cyclone Wind Retrievals from the Advanced Microwave Sounder Unit (AMSU): Application to Surface Wind Analysis. J. of App. Meteor. 45(3), 399-415.

Boukabara, S. A., Garrett, K., Grassotti, C., Iturbide-Sanchez, F., Chen, W., Jiang, Z., Clough, S. A., Zhan, X., Liang, P., Liu, Q., Islam, T., Zubko, V., & Mims, A., 2013, A Physical Approach for a Simultaneous Retrieval of Sounding, Surface, Hydrometeor, and Cryospheric Parameters from SNPP/ATMS. J. of Geophys. Res.Atmos., 118, 12600-12619. [10.1002/2013jd020448]

Bu, Y.P., R.G. Fovell, and K.L. Corbosiero, 2017, The Influences of Boundary Layer Mixing and Cloud-Radiative Forcing on Tropical Cyclone Size. J. Atmos. Sci., 74, 1273–1292, DOI: 10.1175/JAS-D-16-0231.1

Chan, P.W., K.K. Hon and S. Foster, 2011, Wind data collected by a fixed-wing aircraft in the vicinity of a tropical cyclone over the south China coastal waters. Meteorologische Zeitschrift, 20, 313 – 321, DOI: 10.1127/0941-2948/2011/0505.

Christophersen, H., A. Aksoy, J. Dunion, and K. Sellwood, 2017, The Impact of NASA Global Hawk Unmanned Aircraft Dropwindsonde Observations on Tropical Cyclone Track, Intensity, and Structure: Case Studies. Mon. Wea. Rev., 145, 1817–1830, DOI: 10.1175/MWR-D-16-0332.1

Christophersen, H., A. Aksoy, J. Dunion, and S. Aberson, 2018a, Composite Impact of Global Hawk Unmanned Aircraft Dropwindsondes on Tropical Cyclone Analyses and Forecasts. Mon. Wea. Rev., 146, 2297–2314, DOI: 10.1175/MWR-D-17-0304.1

Christophersen, H., R. Atlas, A. Aksoy, and J. Dunion, 2018b, Combined Use of Satellite Observations and Global Hawk Unmanned Aircraft Dropwindsondes for Improved Tropical Cyclone Analyses and Forecasts. Wea. Forecasting, 33, 1021–1031, DOI: 10.1175/WAF-D-17-0167.1

Chirokova, G., M. DeMaria, J. A. Knaff, S. P. Longmore, and J. L. Beven, 2017, ATMS - MiRS: Tropical Cyclone Applications. Clouds Session. JPSS Annual Science Team Meeting, 14-18 August, College Park, MD.

Chou, K.-H., C.-C. Wu, P.-H. Lin, S. D. Aberson, M. Weissmann, F. Harnisch, and T. Nakazawa, 2011, The impact of dropwindsonde observations on typhoon track forecasts in DOTSTAR and T-PARC. Mon. Wea. Rev., 139, 1728–1743.

Cione, J.J., E.A. Kalina, E.W. Uhlhorn, A.M. Farber, and B. Damiano, 2016, Coyote unmanned aircraft system observations in Hurricane Edouard (2014). Earth and Space Science, 3, 370-380, DOI: 10.1002/2016EA000187.

DeMaria, M., R.T. DeMaria, J.A. Knaff, and D. Molenar, 2012, Tropical Cyclone Lightning and Rapid Intensity Change. Mon. Wea. Rev., 140, 1828–1842, DOI: 10.1175/MWR-D-11-00236.1

Demuth, J. L., DeMaria, M., Knaff, J. A., and Vonder Haar, T. H., 2004, Validation of an Advanced Microwave Sounding Unit tropical cyclone intensity and size estimation algorithm, J. Appl. Meteor., 43, 282-296.

Demuth, J.L., M. DeMaria, and J.A. Knaff, 2006, Improvement of Advanced Microwave Sounding Unit tropical cyclone intensity and size estimation algorithms. J. Appl. Meteor., 45, 1573-1581.

Dolling, K., E.A. Ritchie, and J.S. Tyo, 2016, The Use of the Deviation Angle Variance Technique on Geostationary Satellite Imagery to Estimate Tropical Cyclone Size Parameters. Wea. Forecasting, 31, 1625–1642.

Emanuel, K., and R. Rotunno, 2011, Self-stratification of tropical cyclone outflow. Part I: Implications for storm structure, J. Atmos. Sci., 68, 2236–2249, DOI: 10.1175/JAS-D-10-05024.1.

Fore, A.G., Yueh, S.H., Tang, W., Stiles, B.W. and Hayashi, A.K., 2016, Combined active/passive retrievals of ocean vector wind and sea surface salinity with SMAP, IEEE Trans. Geosci. Rem. Sens.,54, 7396-7404, DOI: 10.1109/TGRS.2016.2601486.

Goodman, S. J., and Coauthors, 2013: The GOES-R Geostationary Lightning Mapper (GLM). Atmos. Res., 125–126, 34–49, DOI: 10.1016/j.atmosres.2013.01.006

Gopalakrishnan, S.G., F. Marks, J.A. Zhang, X. Zhang, J. Bao, and V. Tallapragada, 2013, A Study of the Impacts of Vertical Diffusion on the Structure and Intensity of the Tropical Cyclones Using the High-Resolution HWRF System. J. Atmos. Sci., 70, 524–541, DOI: 10.1175/JAS-D-11-0340.1

Horstmann, J., S. Falchetti, C. Wackerman, S. Maresca, M. J. Caruso and H. C. Graber, 2015, Tropical cyclone winds retrieved from C-band cross-polarized synthetic aperture radar, IEEE Trans. Geosci. Remote Sens., vol. 53, no. 5, pp. 2887-2898, 2015.

Hwang, P., and F. Fois, 2015, Surface roughness and breaking wave properties from polarimetric microwave radar backscattering, J. Geophys. Res., 120(C5), 3640-3657, DOI: 10.1002/2015JC010782.

Knaff, J. A., S. P. Longmore, and D. A. Molenar, 2014, An Objective Satellite-Based Tropical Cyclone Size Climatology. J. Climate, 27, 455-476. DOI: 10.1175/JCLI-D-13-00096.1.

Knaff, J. A., C. J. Slocum, K. D. Musgrave, C. R. Sampson, and B. R. Strahl, 2016, Using routinely available information to estimate tropical cyclone wind structure, Mon. Wea. Rev., 144, 1233-1247.

Kishimoto, K., M. Sasaki, and M. Kunitsugu, 2013, Cloud Grid Information Objective Dvorak Analysis (CLOUD) at the RSMC Tokyo - Typhoon Center. Technical Review of RSMC Tokyo-Typhoon Center, 13, 1–15.

Lei, X.T., W.K. Wong, C. Fong, 2017, A Challenge of the Experiment on Typhoon Intensity Change in Coastal Area. Tropical Cyclone Research and Review, 6, 94-97, DOI: 10.6057/2017TCRRh3.04.

Meissner, T., L Ricciardulli, J. Hawkins, M. Kucas, M. Morris, A. Mouche, N. Reul, K. Woods, 2018, Subtopic 7.1: New and Existing Methods to Estimate TC Surface Wind Structure. WMO International Workshop on Tropical Cyclones - 9, Honolulu, HI, USA, 3-7 December, 22pp

Meissner, T., L Ricciardulli, and F.J. Wentz, 2017, Capability of the SMAP Mission to Measure Ocean Surface Winds in Storms, Bulletin of the American Meteorological Society 98(8), 1660-1677, doi: 10.1175/BAMS-D-16-0052.1.

Meissner, T., L. Ricciardulli, and F. Wentz, 2018, Remote Sensing Systems SMAP daily Sea Surface Winds Speeds on 0.25 deg grid, Version 01.0. [NRT or FINAL]. Remote Sensing Systems, Santa Rosa, CA. Available online at www.remss.com/missions/smap/.

Monahan, E., and I. O'Muircheartaigh, 1980, Optimal power-law description of oceanic white-cap coverage dependence on wind speed, J. Phys. Oceanogr., 10, 2094-2099, doi: 10.1175/1520-0485(1980)010<2094:OPLDOO>2.0.CO;2.

Morris, M., and C. S. Ruf, 2017a, Estimating Tropical Cyclone Integrated Kinetic Energy with the CYGNSS Satellite Constellation. J. Appl. Meteor. Climatol., 56, 235–245, doi: 10.1175/JAMC-D-16-0176.1.

Morris, M., and C. S. Ruf, 2017b, Determining Tropical Cyclone Surface Wind Speed Structure and Intensity with the CYGNSS Satellite Constellation, J. Appl. Meteor. Climatol., 56(7), 1847–1865, DOI: 10.1175/JAMC-D-16-0375.1.

Mouche, A., B. Chapron, B. Zhang, and R. Husson, 2017, Combined co- and cross-polarized SAR measurements under extreme wind conditions, IEEE Trans. Geosci. Remote Sens., 99, Aug. 2017.

Neumann, C. J., 1952, Wind estimations from aerial observations of sea conditions. Weather Squadron Two (VJ-2) Rep., 29 pp., available online at http://www.aoml.noaa.gov/hrd/hurdat/seastate-aircraft.pdf.

Nordberg, W., J. Conaway, D. Ross, and T. Wilheit, 1971, Measurement of microwave emission from a foam covered wind driven sea, J. Atmos. Sci., 38, 429-433, DOI: 10.1175/1520-0469(1971)028<0429:MOMEFA>2.0.CO;2.

Olander, T. and C. Velden, 2018, The UW-CIMSS Advanced Dvorak Technique (ADT) - current status and future upgrades. 33rd AMS Conference on Hurricanes and Tropical Meteorology, Ponte Vedra, FL, Abstract 247.

Oyama, R., M. Sawada, K Shimoji, 2018, Diagnosis of Tropical Cyclone Intensity and Structure Using Upper Tropospheric Atmospheric Motion Vectors. Journal of the Meteorological Society of Japan. Ser. II, Volume 96B, Pages 3-26. DOI: 10.2151/jmsj.2017-024.

Piñeros, M. F., E. A. Ritchie, and J. S. Tyo, 2008, Objective measures of tropical cyclone structure and intensity change from remotely-sensed infrared image data. IEEE Trans. Geosci. Remote Sens., 46, 3574–3580.

Reul, N., and B. Chapron, 2003, A model of sea-foam thickness distribution for passive micro-wave remote sensing applications, J. Geophys. Res., 108(C10), DOI: 10.1029/2003JC001887.

Reul, N., J. Tenerelli, B. Chapron, D. Vandemark, Y. Quilfen, and Y. Kerr, 2012, SMOS satellite L-band radiometer: A new capability for ocean surface remote sensing in hurricanes. J. Geophys. Res., 117, C02006, DOI: 10.1029/2011JC007474.

Reul, N., B. Chapron, E. Zabolotskikh, C. Donlon, Y. Quilfen, S. Guimbard and J. F. Piolle, 2016, A revised L-band radio-brightness sensitivity to extreme winds under Tropical Cyclones: the five year SMOS-storm database. Remote Sens. Environ., 180, 274-291, DOI: 10.1016/j.rse.2016.03.011.

Rogers, R.F., S.D. Aberson, M.L. Black, P. Black, J. Cione, P. Dodge, J. Dunion, J. Gamache, J. Kaplan, M. Powell, N. Shay, N. Surgi, and E. Uhlhorn, 2006, The Intensity Forecasting Experiment (IFEX): A NOAA Multi-Year Field Program for Improving Tropical Cyclone Intensity Forecasts. Bulletin of the American Meteorological Society, 87, 1523-1537

Rogers, R.F., S.Aberson, A. Aksoy, B. Annane, M. Black, J. Cione, N. Dorst, J. Dunion, J. Gamache, S. Goldenberg, S. Gopalakrishnan, J. Kaplan, B. Klotz, S. Lorsolo, F. Marks, S. Murillo, M. Powell, P. Reasor, K. Sellwood, E. Uhlhorn, T. Vukicevic, J. Zhang, and X. Zhang, 2013, NOAA'S Hurricane Intensity Forecasting Experiment: A Progress Report. Bull. Amer. Meteor. Soc., 94, 859–882.

Ruf, C. S., R. Atlas, P. S. Chang, M. P. Clarizia, J. L. Garrison, S. Gleason, S. J. Katzberg, Z. Jelenak, J. T. Johnson, S. J. Majumdar, A. O’Brien, D. J. Posselt, A. J. Ridley, R. J. Rose, V. U. Zavorotny, 2016a, New Ocean Winds Satellite Mission to Probe Hurricanes and Tropical Convection, Bull. Amer. Meteor. Soc., DOI:10.1175/BAMS-D-14-00218.1.

Ruf, C., P. Chang, M.P. Clarizia, S. Gleason, Z. Jelenak, J. Murray, M. Morris, S. Musko, D. Posselt, D. Provost, D. Starkenburg, V. Zavorotny, 2016b, CYGNSS Handbook, Ann Arbor, MI, Michigan Pub., ISBN 978-1-60785-380-0, 154 pp, 1 Apr 2016.

Ruf, C. and R. Balasubramaniam, 2018, Development of the CYGNSS Geophysical Model Function for Wind Speed, IEEE J. Sel. Topics Appl. Earth Obs. Remote Sens., DOI: 10.1109/JSTARS.2018.2833075.

Ruf, C.S., C. Chew, T. Lang, M.G. Morris, K. Nave, A. Ridley, R. Balasubramaniam, 2018, A New Paradigm in Earth Environmental Monitoring with the CYGNSS Small Satellite Constellation. Scientific Reports, DOI: 10.1038/s41598-018-27127-4.

Sampson, C.R. and A.J. Schrader, 2000, The Automated Tropical Cyclone Forecasting System (version 3.2), Bull. Amer. Meteor. Soc., 81, 1231–1240.

Sampson, C.R., E.M. Fukada, J.A. Knaff, B.R. Strahl, M.J. Brennan, and T. Marchok, 2017, Tropical cyclone gale wind radii estimates for the western North Pacific, Wea. Forecasting, 32, 1029–1040.

Sampson, C. R., J. S. Goerss, J. A. Knaff, B. R. Strahl, E. M. Fukada, E. A. Serra, 2018, Tropical cyclone gale wind radii estimates, forecasts and error forecast for the western North Pacific, Wea. Forecasting, 33, 1081-1092.Zavorotny, V. U., S. Gleason, E. Cardellach and A. Camps, 2014, Tutorial on remote sensing using GNSS bistatic radar of opportunity. IEEE Geosci. Remote Sens., 2, 8–45, DOI:10.1109/MGRS.2014.2374220

Stevenson, S.N., K.L. Corbosiero, M. DeMaria, and J.L. Vigh, 2018, A 10-Year Survey of Tropical Cyclone Inner-Core Lightning Bursts and Their Relationship to Intensity Change. Wea. Forecasting, 33, 23–36, DOI: 10.1175/WAF-D-17-0096.1

Tong, M., J.A. Sippel, V. Tallapragada, E. Liu, C. Kieu, I. Kwon, W. Wang, Q. Liu, Y. Ling, and B. Zhang, 2018, Impact of Assimilating Aircraft Reconnaissance Observations on Tropical Cyclone Initialization and Prediction using Operational HWRF and GSI Ensemble-Variational Hybrid Data Assimilation. Mon. Wea. Rev., DOI: 10.1175/MWR-D-17-0380.1

Torn, R.D., 2014, The Impact of Targeted Dropwindsonde Observations on Tropical Cyclone Intensity Forecasts of Four Weak Systems during PREDICT. Mon. Wea. Rev., 142, 2860–2878, DOI: 10.1175/MWR-D-13-00284.1

Weng, Y. and F. Zhang, 2016, Advances in convection-permitting tropical cyclone analysis and prediction through EnKF assimilation of reconnaissance aircraft observations. J. Met. Soc. Japan, 94, 345-358.

Wong, W. K., S.M. Tse and P.W. Chan., 2014, Impacts of reconnaissance flight data on numerical simulation of tropical cyclones over South China Sea. Met. Apps, 21: 831-847. DOI:10.1002/met.1412.

Wong, W.K., P. Black, K. Ito, X. Lei, P-H Lin, R. Rogers, K. Tsuboki, C-C Wu, 2018, Subtopic 7.3: New Developments and Science Using Aircraft-based Reconnaissance. WMO International Workshop on Tropical Cyclones - 9, Honolulu, HI, USA, 3-7 December, 15pp

Zavorotny, V. U., S. Gleason, E. Cardellach and A. Camps, 2014, Tutorial on remote sensing using GNSS bistatic radar of opportunity. IEEE Geosci. Remote Sens., 2, 8–45, DOI: 10.1109/MGRS.2014.2374220.

Zhang, B. and W. Perrie, 2012, Cross-polarized synthetic aperture radar: A new potential measurement technique for hurricanes, Bull. Am. Meterol. Soc., vol. 93, no. 4, pp. 531-541, Apr. 2012.

Zhang, J. A., S. G. Gopalakrishnan, F. D. Marks, R. F. Rogers, and V. Tallapragada, 2013a, A Developmental Framework for Improving Hurricane Model Physical Parameterizations Using Aircraft Observations. Trop. Cycl. Res. Rev, 1(4), 419-429

Zhang, J.A., R.F. Rogers, P. Reasor, E. Uhlhorn, and F.D. Marks, Jr., 2013b, Asymmetric hurricane boundary layer structure from dropsonde composites in relation to the environmental wind shear. Mon. Wea. Rev., 141, 3968–3984

Zhang, J.A., D.S. Nolan, R.F. Rogers, and V. Tallapragada, 2015, Evaluating the Impact of Improvements in the Boundary Layer Parameterization on Hurricane Intensity and Structure Forecasts in HWRF. Mon. Wea. Rev., 143, 3136-3155

Zhang, J.A., R.F. Rogers, and V. Tallapragada, 2017, Impact of Parameterized Boundary Layer Structure on Tropical Cyclone Rapid Intensification Forecasts in HWRF. Mon. Wea. Rev., 145, 1413–1426, DOI: 10.1175/MWR-D-16-0129.1

Zhang, J.A., F.D. Marks, J.A. Sippel, R.F. Rogers, X. Zhang, S.G. Gopalakrishnan, Z. Zhang, and V. Tallapragada, 2018, Evaluating the Impact of Improvement in the Horizontal Diffusion Parameterization on Hurricane Prediction in the Operational

Hurricane Weather Research and Forecast (HWRF) Model. Wea. Forecasting, 33, 317–329, DOI: 10.1175/WAF-D-17-0097.1

Zhang, F. and Y. Weng, 2015: Predicting Hurricane Intensity and Associated Hazards: A Five-Year Real-Time Forecast Experiment with Assimilation of Airborne Doppler Radar Observations. Bull. Amer. Meteor. Soc., 96, 25–33, DOI: 10.1175/BAMS-D-13-00231.1